

Phosphorescence and Structure of a Tetrameric Copper(I)–Amide Cluster

Alicia M. James, Ravi K. Laxman, Frank R. Fronczek, and Andrew W. Maverick*

Department of Chemistry, Louisiana State University, Baton Rouge, Louisiana 70803-1804

Received October 22, 1997

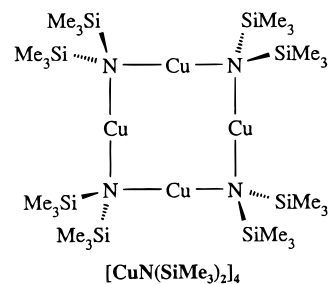
The colorless copper(I) cluster $[\text{CuN}(\text{Si}(\text{CH}_3)_2)_4]$, which contains a square-planar Cu_4N_4 core, phosphoresces in CH_2Cl_2 solution (λ_{max} , 512 nm; lifetime, 30 μs) and in the solid state at room temperature. Its electronic absorption spectrum in CH_2Cl_2 consists of two intense bands at 283 and 246 nm; these transitions, as well as the phosphorescence, are likely to involve population of MOs reflecting substantial $\text{Cu}\cdots\text{Cu}$ interactions. Solid $[\text{CuN}(\text{Si}(\text{CH}_3)_2)_4]$ luminesces with approximately the same spectrum as that of the CH_2Cl_2 solutions. At 77 K, the solid-state luminescence red-shifts slightly (λ_{max} , 524 nm) and narrows substantially (fwhm, 2400 cm^{-1} ; vs 3500 cm^{-1} at 300 K); the emission lifetime in glassy Et_2O solution is 690 μs . X-ray analysis of crystals of $[\text{CuN}(\text{Si}(\text{CH}_3)_2)_4]$ at 130 and 296 K shows that, although the previously reported structure solution (in space group $I2/m$, with the molecules on $2/m$ sites; *Eur. J. Solid State Inorg. Chem.* **1992**, *29*, 573–583) is approximately correct, the lattice is actually primitive, $P2/n$, and the only crystallographically required symmetry element for the molecule is a 2-fold axis. $\text{C}_{24}\text{H}_{72}\text{Cu}_4\text{N}_4\text{Si}_8$: monoclinic, space group $P2/n$, $Z = 2$. At 130 K, $a = 9.285(3)$ Å, $b = 13.393(3)$ Å, $c = 17.752(5)$ Å, and $\beta = 90.53(2)^\circ$. [At 296 K, $a = 9.3773(4)$ Å, $b = 13.5836(7)$ Å, $c = 17.814(2)$ Å, and $\beta = 90.207(7)^\circ$.] At 130 K, the Cu and N atoms in the cluster are planar within 0.007 Å, and the Cu–N and Cu \cdots Cu distances are 1.917(4)–1.925(4) and 2.6770(7)–2.6937(7) Å, respectively. Despite the low volatility of the compound, it can be used as a precursor for chemical vapor deposition (CVD) of copper metal, under H_2 carrier gas, with both source and substrate at ca. 200 °C. Smaller amounts of Cu metal films are also deposited when the substrate temperature is as low as 145 °C (in the dark) or 136–138 °C (under Pyrex-filtered Xe arc lamp illumination). Thus, Cu CVD with this precursor shows slight photochemical enhancement.

Introduction

Numerous volatile copper(I) complexes have been examined in recent years as possible precursors for the chemical vapor deposition (CVD) of copper metal.¹ The family of species $(\text{hfac})\text{CuL}$ ($\text{L} =$ neutral ligand)² has been most intensively studied; other copper(I) precursors include $[\text{CuOCMe}_3]_4$ ³ and CpCuPEt_3 ($\text{Cp} =$ cyclopentadienyl).⁴

We have been interested in volatile copper complexes that also show photochemical activity, so that Cu deposition might be induced by light.⁵ Several studies of laser-induced Cu CVD have been reported.^{6–11} However, these experiments have generally utilized high-energy laser sources, so that both photochemical (i.e. via laser-induced heating of the substrate) and photochemical processes have been observed. We wished to take advantage of copper(I) complexes that possess well-defined low-energy excited states, which might react more cleanly with reducing carrier gases to produce pure Cu. Although numerous copper(I) complexes are known to show photochemical activity,¹² many of these are ions (e.g. $\text{Cu}(\text{Me}_2\text{phen})_2^+$, $\text{Cu}(\text{phen})(\text{PPh}_3)_2^+$) whose salts are of low volatility. In contrast, neutral

metal amide complexes, especially those containing the bis-(trimethylsilyl)amide ligand $(\text{SiMe}_3)_2\text{N}^-$, are often distillable or sublimable.¹³ We now report that the planar tetrameric copper(I) cluster $[\text{CuN}(\text{SiMe}_3)_2]_4$ is both luminescent and



sufficiently volatile for CVD of Cu films. Chisholm et al. have recently reported the use of $[\text{CuN}(\text{SiMe}_3)_2]_4$ as a precursor for Cu CVD.¹⁴ However, their depositions were performed at 275

- (1) Hampden-Smith, M. J.; Kodas, T. T. In *The Chemistry of Metal CVD*; Kodas, T. T., Hampden-Smith, M. J., Eds.; VCH: Weinheim, Germany, 1994; Chapter 5.
- (2) Ligand abbreviations: hfacH = 1,1,1,5,5,5-hexafluoro-2,4-pentanedione; phen = 1,10-phenanthroline; $\text{Me}_2\text{phen} = 2,9$ -dimethyl-1,10-phenanthroline; dppe = $\text{Ph}_2\text{PCH}_2\text{CH}_2\text{PPh}_2$.
- (3) Jeffries, P. M.; Girolami, G. S. *Chem. Mater.* **1989**, *1*, 8–10.
- (4) Beach, D. B.; LeGoues, F. K.; Hu, C.-K. *Chem. Mater.* **1990**, *2*, 216–219.
- (5) For a discussion of applications and techniques of light-induced thin film deposition, see: Ibbs, K. G.; Osgood, R. M., Eds. *Laser Chemical Processing for Microelectronics*; Cambridge University Press: Cambridge, U.K., 1989.

- (6) Dupuy, C. G.; Beach, D. B.; Hurst, J. E., Jr.; Jasinski, J. M. *Chem. Mater.* **1989**, *1*, 16–18.
- (7) Jones, C. R.; Houle, F. A.; Kovac, C. A.; Baum, T. H. *Appl. Phys. Lett.* **1985**, *46*, 97–99. Wilson, R. J.; Houle, F. A. *Phys. Rev. Lett.* **1985**, *55*, 2184–2187.
- (8) Houle, F. A.; Wilson, R. J.; Baum, T. H. *J. Vac. Sci. Technol.* **1986**, *A4*, 2452–2458.
- (9) Markwalder, B.; Widmer, M.; Braichotte, D.; Van den Bergh, H. J. *Appl. Phys.* **1989**, *65*, 2470–2474.
- (10) Han, J.; Jensen, K. F. *J. Appl. Phys.* **1994**, *75*, 2240–2250.
- (11) Chen, Y. D.; Reisman, A.; Turlik, I.; Temple, D. *J. Electrochem. Soc.* **1995**, *142*, 3911–3918.
- (12) Kutal, C. *Coord. Chem. Rev.* **1990**, *99*, 213–252.
- (13) Lappert, M. F.; Power, P. P.; Sanger, A. R.; Srivastava, R. C. *Metal and Metalloid Amides*; Horwood: Chichester, England, 1980.

°C, whereas we show that Cu films form at substrate temperatures as low as 145 °C. In addition, we find a slightly lower threshold temperature for Cu CVD with this precursor under Xe arc lamp irradiation.

Also presented here is the crystal structure of $[\text{CuN}(\text{SiMe}_3)_2]_4$. An X-ray analysis of this compound has been reported by Miele et al.¹⁵ Our low-temperature data and lower-symmetry space group reveal a more precise and chemically more reasonable structure. An early X-ray study of the cluster, indicating its square-planar shape, was cited in 1980.¹⁶ However, except for the Cu···Cu distance of 2.685 Å,¹⁷ no details from that study appear to have been published.

Experimental Section

Materials and Procedures. Reagents were obtained from Aldrich Chemical Co. Solvents were HPLC or spectrophotometric grade and were used without further purification, except for tetrahydrofuran (THF), which was distilled from sodium/benzophenone before use.

Preparation of $[\text{CuN}(\text{SiMe}_3)_2]_4$ from CuCl. A solution of NaN(SiMe₃)₂ (1 M; 5 mL) in THF was added dropwise to a suspension of CuCl (0.50 g, 5 mmol) in THF in a drybox, with stirring. After all of the sodium salt had been added, the mixture was stirred for 30 min, refluxed under N₂ for 1 h, and evaporated to dryness and the yellow-brown residue stirred with CH₂Cl₂–pentane (1:1 (v/v), 40 mL). The resulting suspension was filtered to remove insoluble material and evaporated. If the residue was still colored, the extraction–filtration–evaporation procedure was repeated. Yield of colorless crystalline powder: 65–70%. NMR (CDCl₃, vs tetramethylsilane (TMS)): ¹H, 0.35 ppm (200 MHz; lit.¹⁸ 0.34 ppm); ¹³C, 7.8 ppm (50 MHz). X-ray quality crystals of $[\text{CuN}(\text{SiMe}_3)_2]_4$ were grown over a period of several days by layering a THF solution of LiN(SiMe₃)₂ on a mixture of THF and CuCl.

Reactivity of CuCl₂ with (SiMe₃)₂N⁻. Solid LiN(SiMe₃)₂ (1–2 equiv) was added to a suspension of anhydrous CuCl₂ in THF, causing the color to change quickly to purple. After the lithium salt had been added, the solvent was removed, at which point the color changed from purple to green. Attempts to isolate tractable copper(II) complexes from the purple and green materials failed, but if the solutions are refluxed and allowed to cool, a solid containing $[\text{CuN}(\text{SiMe}_3)_2]_4$ precipitates.

Photophysical Data. Electronic absorption and corrected phosphorescence spectra were recorded by using Aviv Model 14DS and Spex Instruments Fluorolog 2 Model F112X (Hamamatsu R928 or R636 PMT) instruments, respectively. An Oxford Instruments Model DN1704 cryostat was employed for low-temperature measurements. Lifetime measurements employed a Laser Photonics N₂ laser (337 nm; pulse width < 1 ns; energy, 1 mJ) as excitation source, and colored-glass filters and a McPherson ¹/₄ m monochromator to isolate the emitted light. The emission signal from the photomultiplier tube (Hamamatsu R928) was passed to a Hewlett-Packard Model 54111D digitizing oscilloscope. Lifetimes were determined by exponential fits to the digitized phosphorescence decay curves, after subtraction of dark current.

X-ray analysis. Diffraction data (see summary in Table 1) were collected on Enraf-Nonius CAD4 diffractometers fitted with Cu Kα (room temperature) or Mo Kα (130 K) sources and graphite monochromators, using the θ – 2θ scan method. Final unit cell constants were determined from the orientations of 25 centered high-angle

Table 1. Crystal Data for $[\text{CuN}(\text{SiMe}_3)_2]_4^a$

formula	C ₂₄ H ₇₂ Cu ₄ Si ₈ N ₄	
fw	895.7	
space group	P2/n	
Z	2	
a/Å	9.285(3)	9.3773(4)
b/Å	13.393(3)	13.5836(7)
c/Å	17.752(5)	17.814(2)
β/deg	90.53(2)	90.207(7)
V/Å ³	2208(2)	2269.1(5)
T/K	130	296 ^b
λ/Å	0.710 73 (Mo Kα)	1.541 84 (Cu Kα)
ρ _{calc} /g cm ⁻³	1.347	1.311
μ/cm ⁻¹	21.4	43.1
R(F) (obsd data) ^c	0.061	0.040
R _w (F) ^d	0.041	0.044

^a In Tables 1–3, estimated standard deviations in the least significant digits of the values are given in parentheses. ^b Complete results available in electronic form. ^c $R = \sum ||F_o| - |F_c|| / \sum |F_o|$; data with $I > 1\sigma(I)$. ^d $R_w = [(\sum w(|F_o| - |F_c|)^2) / \sum w F_o^2]^{1/2}$; $w = 4F_o^2 / (\sigma^2(I) + (0.02F_o)^2)$.

reflections. The intensities were corrected for absorption using ψ scan data (five reflections measured for each data set). For the 130 K data set, the crystal was cooled in a thermostated N₂ cold stream. The MolEN¹⁹ set of programs was used for structure solution and refinement.

Once the most likely space group for these crystals, P2/n, was chosen (see below), the Cu, Si, and N coordinates from the other attempts were used as the starting point for solution. The coordinates from our own trials in P2₁/n, and those from the previously published analysis in I2/m,¹⁵ had to be translated by ¹/₄, ¹/₄, ¹/₄, for proper placement with respect to the symmetry elements of P2/n. Structure factors calculated using the Cu, Si, and N positions did not phase the weak reflections well, as those atoms lie in a pseudo-body-centered array. Difference Fourier methods with this model led to no real improvement over previous models. However, starting with the Cu₄N₄Si₈ core, DIRDIF²⁰ successfully located almost all C atoms. Others were placed in calculated positions. Refinement was carried out using $I > 1\sigma(I)$ data in order to include more weak data, which are needed to define the C positions. Refinement proceeded smoothly despite the hypercentric nature of the structure. The $h+k+l$ -odd data were fit well considering their low intensity: $R = 0.19$ and $R = 0.071$ for data at 130 and 296 K, respectively. Refinement of H atom coordinates was almost completely successful, with most of them ending up in quite reasonable positions; it was clear that the conformation of all of the CH₃ groups was the expected staggered one. However, since some refined H atom positions gave slightly long C–H distances (1.1–1.2 Å), all H atoms were placed in calculated positions in the final refinements, with C–H 0.95 Å and $U_{\text{iso}} = 1.3 U_{\text{eq}}$ for the attached C atoms. Atomic positions and selected distances and angles for the 130 K structure are in Tables 2 and 3. Complete X-ray results are available as CIF files via the Internet.

CVD experiments were performed under 1 atm H₂, with a flow rate of 100 mL min⁻¹. In initial experiments, the $[\text{CuN}(\text{SiMe}_3)_2]_4$ precursor was placed in a borosilicate glass tube inside a tube furnace, and H₂ was passed through the tube. For each CVD experiment using this apparatus, the furnace was warmed to a constant temperature while H₂ was passed over the precursor; passage of H₂ was continued for 30 min while the reactor was at temperature, and also during a subsequent cooling period (ca. 1 h).

To prepare Cu films suitable for analysis by X-ray powder diffraction, we also carried out depositions in a warm-wall pedestal reactor²¹ with an upward-facing pedestal. For these experiments,

- (14) Baxter, D. V.; Chisholm, M. H.; Gama, G. J.; Hector, A. L.; Parkin, I. P. *Adv. Mater.* **1995**, *7*, 49–51.
 (15) Miele, P.; Foulon, J. D.; Hovnanian, N.; Durand, J.; Cot, L. *Eur. J. Solid State Inorg. Chem.* **1992**, *29*, 573–583.
 (16) Hursthouse, M. B. Personal communication. Cited In: Lappert, M. F.; Power, P. P.; Sanger, A. R.; Srivastava, R. C. *Metal and Metalloid Amides*; Horwood: Chichester, England, 1980; p 493.
 (17) Bradley, D. C. Unpublished work. Cited In: ten Hoedt, R. W. M.; Noltes, J. G.; van Koten, G.; Spek, A. L. *J. Chem. Soc., Dalton Trans.* **1978**, 1800–1806.
 (18) Bürger, H.; Wannagat, U. *Monatsh. Chem.* **1964**, *95*, 1099–1102.

- (19) Fair, C. K. *MolEN: An Interactive Structure Solution Procedure*; Enraf-Nonius: Delft, The Netherlands, 1990.
 (20) Beurskens, P. T. *DirDif: Technical Report 1984/1*; Crystallography Laboratory, Toernooiveld, Nijmegen, The Netherlands, 1984.
 (21) This reactor is similar to one we have used previously (Kumar, R.; Fronczek, F. R.; Maverick, A. W.; Lai, W. G.; Griffin, G. L. *Chem. Mater.* **1992**, *4*, 577–582), except that its susceptor is 2.5 cm in diameter.

Table 2. Atomic Coordinates for $[\text{CuN}(\text{SiMe}_3)_2]_4$ at 130 K

	<i>x</i>	<i>y</i>	<i>z</i>	$U_{\text{eq}}/\text{\AA}^2$
Cu1	0.29415(5)	0.34872(4)	0.17794(3)	0.0161(1)
Cu2	0.29474(5)	0.14884(4)	0.17821(3)	0.01496(9)
Si1	0.5255(1)	0.2554(1)	0.08604(5)	0.0189(2)
Si2	0.2202(1)	0.2396(1)	0.02694(6)	0.0204(2)
Si3	0.1017(1)	0.5185(1)	0.21481(7)	0.0243(3)
Si4	0.0942(1)	−0.02125(9)	0.22401(6)	0.0178(3)
N1	0.3389(3)	0.2483(3)	0.1042(1)	0.0152(6)
N2	$1/4$	0.4506(3)	$1/4$	0.016(1)
N3	$1/4$	0.0461(4)	$1/4$	0.018(1)
C1	0.6315(4)	0.2201(3)	0.1709(3)	0.026(1)
C2	0.5831(5)	0.1678(4)	0.0110(3)	0.040(1)
C3	0.5817(5)	0.3839(4)	0.0580(3)	0.032(1)
C4	0.0339(5)	0.2784(3)	0.0520(3)	0.029(1)
C5	0.2130(5)	0.1092(4)	−0.0096(3)	0.033(1)
C6	0.2731(5)	0.3227(4)	−0.0527(3)	0.037(1)
C7	0.0542(6)	0.6264(4)	0.2765(3)	0.044(1)
C8	−0.0640(5)	0.4408(4)	0.2102(3)	0.037(1)
C9	0.1360(5)	0.5654(4)	0.1177(3)	0.038(1)
C10	−0.0331(5)	0.0578(4)	0.1692(3)	0.027(1)
C11	−0.0042(5)	−0.0691(4)	0.3078(3)	0.028(1)
C12	0.1376(5)	−0.1296(3)	0.1613(3)	0.027(1)

$^a U_{\text{eq}} = 1/3[a^2(a^*)^2U_{11} + b^2(b^*)^2U_{22} + c^2(c^*)^2U_{33} + 2aca^*c^*U_{13} \cos \beta]$.

Table 3. Selected Interatomic Distances (Å) and Angles (deg) for $[\text{CuN}(\text{SiMe}_3)_2]_4$ at 130 K^a

Cu1...Cu1'	2.6937(7)
Cu1...Cu2	2.6770(7)
Cu1–N1	1.925(4)
Cu1–N2	1.917(3)
Cu2...Cu2'	2.6883(7)
Cu2–N1	1.917(4)
Cu2–N3	1.924(3)
Si1–N1	1.768(3)
Si2–N1	1.756(3)
Si3–N2	1.760(3)
Si4–N3	1.763(3)
Si–C	1.853(4)–1.875(5)
N1–Cu1–N2	179.0(1)
N1–Cu2–N3	178.3(1)
Cu1–N1–Cu2	88.3(1)
Cu1–N1–Si1	107.7(2)
Cu1–N1–Si2	116.1(2)
Cu2–N1–Si1	112.3(2)
Cu2–N1–Si2	110.6(2)
Si1–N1–Si2	118.0(1)
Cu1–N2–Cu1'	89.3(2)
Cu1–N2–Si3	107.61(6)
Cu1–N2–Si3'	115.69(6)
Si3–N2–Si3'	117.7(3)
Cu2–N3–Cu2'	88.7(2)
Cu2–N3–Si4	111.99(6)
Cu2–N3–Si4'	110.96(6)
Si4–N3–Si4'	118.4(3)

^a Primes refer to atoms related by the symmetry operation $1/2-x, y, 1/2-z$.

because we anticipated that transporting the precursor from a separate flask to the substrate would be difficult, we placed the powdered solid precursor in the center of the substrate. Deposition then occurred on the substrate beneath and around the precursor. The films were analyzed by using a Siemens automated powder diffractometer. Photoinduced depositions were carried out with the same apparatus, but with the beam from a Kratos/Schoeffel 150 W Xe arc lamp focused through the Pyrex housing ($\lambda > \sim 300$ nm) onto the substrate. The surface temperature of the substrate was monitored during the photochemical experiments to ensure that there was no significant rise in temperature caused by the arc lamp.

Results

Synthesis and Properties. The tetranuclear copper(I) cluster $[\text{CuN}(\text{SiMe}_3)_2]_4$ studied here is a colorless, crystalline compound first reported by Bürger and Wannagat in 1964.¹⁸ It is stable in air in the solid state for weeks, discoloring to pale blue over longer periods. The cluster is soluble in solvents such as $\text{CH}_2\text{-Cl}_2$, ether, and THF and sparingly soluble in pentane. These solutions are somewhat air-sensitive, but they can be prepared in air without significant decomposition if they are degassed (e.g. by bubbling with N_2) soon after preparation.

CuI and CuCl_2 were used as starting materials in the original preparation of the cluster.¹⁸ We found that CuCl is also a satisfactory starting material. In addition, we were interested in the reactivity of copper(II) with $(\text{SiMe}_3)_2\text{N}^-$: if “ $\text{Cu}^{\text{II}}\text{N}(\text{SiMe}_3)_2$ ” tetramerizes to make the $[\text{CuN}(\text{SiMe}_3)_2]_4$ cluster primarily in order to achieve a higher coordination number about Cu, then perhaps a mononuclear, and therefore more volatile, $\text{Cu}^{\text{II}}(\text{N}(\text{SiMe}_3)_2)_2$ complex would be isolable. In our experiments, adding $\text{LiN}(\text{SiMe}_3)_2$ to a suspension of CuCl_2 in THF led to the formation of a dark purple color. Since many copper(II) complexes with nitrogen coordination are purple, we thought this color might be due to a Cu(II)– $\text{N}(\text{SiMe}_3)_2$ complex. However, we were unable to isolate any well-behaved Cu(II) complexes from these solutions; instead, like the original authors, we found that they contained some of the copper(I) cluster $[\text{CuN}(\text{SiMe}_3)_2]_4$.

Crystal-Structure Solution. $[\text{CuN}(\text{SiMe}_3)_2]_4$ crystallizes in the space group $P2_1/n$, with the molecules lying on crystallographic 2-fold axes. The structure is isomorphous with the reported $P2_1/n$ polymorph of $[\text{AgN}(\text{SiMe}_3)_2]_4$.²²

Since the $0k0$ reflections with k odd are extremely weak for these crystals, we initially considered them to be systematically absent. This would require the space group to be the very common $P2_1/n$. Our attempts to solve the structure in $P2_1/n$ appeared to give satisfactory placement of Cu, N, and Si atoms, although one diagonal of the cluster was aligned very closely along b , which led to some surprising coincidences in coordinates. In other respects, the $P2_1/n$ structure was poor, with large C atom displacement parameters, chemically unreasonable Si–C distances, and $R = 0.12$ ($I > 3\sigma(I)$). (The $h+k+l$ -odd data were particularly poorly fit, with $R = 0.56$ for 1456 reflections.) Use of low-temperature data, recorded for a second crystal, led to little improvement.

Our diffraction data clearly show that the compound crystallizes in a primitive lattice. However, the $h+k+l$ -odd reflections are systematically weak, with average $E^2 = 0.1$, as compared to 1.8 for the $h+k+l$ -even reflections; thus, the structure can be called “pseudo-body-centered”. Thus, either with a smaller crystal or with a room temperature Mo K α data set, one might conclude that the lattice is body-centered; this appears to be what Miele et al.¹⁵ did in their previous study of the compound. Indeed, we were able to duplicate their results by using only $h+k+l$ -even data from our crystal and refining their model in $I2/m$. The $2/m$ molecular symmetry in their model (in particular, the mirror plane, which passed diagonally through the molecule, and contained two N, four Si, and two C atoms, corresponding to N1, Si1, Si2, C2, C6, and their 2-fold-axis-related equivalents N1', Si1', ..., in Figure 1) led to some relatively short C...C nonbonded contacts (3.308 Å) between the two SiMe_3 groups on the same N atom (vs 3.343 Å for C...C between SiMe_3 groups without the mirror constraint; see below). However, their

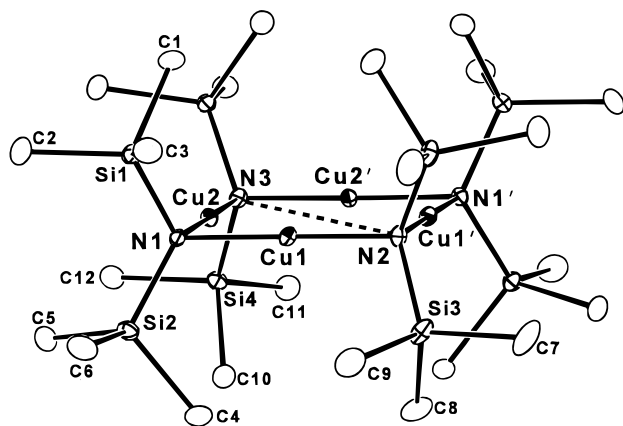


Figure 1. Ortep²⁵ drawing of [CuN(SiMe₃)₂]₄ from 130 K data, with thermal ellipsoids at the 50% probability level. H atoms omitted for clarity. Dashed line shows crystallographically imposed 2-fold axis.

fairly successful placement of the molecule on a $2/m$ site ($R = 0.049$) suggested that other space groups might be better if they permitted different cluster site symmetry, e.g. 2-fold, rather than inversion or $2/m$.

In a recent survey of space-group frequencies, Brock and Dunitz²³ found that, in the most common space groups that contain both inversion centers and 2-fold axes ($C2/c$, $Pccn$, and $Pbcn$), sites of 2-fold symmetry were favored over inversion centers by about a factor of 4. We therefore considered $P2/c$ (in its alternative setting of $P2/n$) as a viable space group, particularly since Brock and Dunitz report that $Z = 2$ occurs 56% of the time in $P2/c$. In a somewhat smaller compilation, Chernikova et al.²⁴ found that, of 12 structures in $P2/c$ with $Z = 2$, a molecule occupied the 2-fold axis in ten and the inversion center in only two.

We reexamined the $0k0$ (k odd) reflections in our data, to judge whether the 2_1 axis in our original $P2_1/n$ assignment is actually present. The weaker 130 K Mo data provided only one reflection, the 050, with $I/\sigma(I) = 3.0$, as a possible violation, but the room temperature Cu data set provided three candidates: 010 with $I/\sigma(I) = 10.2$, 030 with $I/\sigma(I) = 5.3$, and 090 with $I/\sigma(I) = 4.2$. These reflections suggested that the 2_1 axis is absent. We therefore attempted to solve the structure in $P2/n$, with the 2-fold axis passing through opposite N atoms. This model was much more successful (see Experimental Section), and the resulting refined structure is discussed below.

Structure of the Cluster. [CuN(SiMe₃)₂]₄ contains an approximately square Cu₄N₄ core, with the Cu atoms at the centers of the sides, and N atoms of the N(SiMe₃)₂ groups at the corners. The symmetry of the Cu₄N₄Si₈ portion of the cluster is approximately D_{4h} ($4/mmm$); the Cu₄N₄ core of the cluster is planar within 0.007 Å. However, as mentioned above, only 2-fold rotational symmetry is crystallographically required; the 2-fold axis passes through N2 and N3. An ORTEP²⁵ drawing of the molecule appears in Figure 1.

Figure 1 shows a slight twisting of the trimethylsilyl groups away from the orientations of highest possible symmetry. At each N atom, if the two Me₃Si groups were perfectly staggered with respect to the other substituents, there would be close nonbonded contacts between two pairs of methyl groups. These

close contacts include C2...C5 and C3...C6, as well as between C7, C9, C11, and C12 and their symmetry-related counterparts C7', C9', C11', and C12'. Indeed, in the previously reported structure analysis of [CuN(SiMe₃)₂]₄,¹⁵ where the molecular symmetry was required to be C_{2h} ($2/m$), the mirror plane imposed a requirement of an essentially perfectly eclipsed conformation on the methyl groups at Si1 and Si2 and constrained the conformation of the other methyl groups as well. One result of these requirements was close contacts between nonbonded C atoms (3.308 and 3.343 Å). However, in the present determination, the molecule has only 2-fold symmetry. This allows the SiMe₃ groups to twist slightly, so that the shortest intramolecular contact of this type is now C7...C9' (3.518 Å). The amount of twisting in the SiMe₃ groups is approximately 20°, as illustrated by the following torsion angles in our structure: C1–Si1–N1–Si2, –160.3(3)°; C4–Si2–N1–Si1, –159.4(3)°; C8–Si3–N2–Si3', –160.9(3)°; C10–Si4–N3–Si4', –160.8(3)°. The corresponding torsion angles in the previous X-ray analysis¹⁵ are +180, +180, +178.6, and –178.6°; the last two of these angles are required to have opposite signs because the two N(SiMe₃)₂ groups centered at N2 and N3 in $P2/n$ are related by the mirror plane in $I2/m$. The twisting does not constitute a large deviation from staggered conformations at the Si–N bonds, yet it reduces the unfavorable C...C interactions.

All of the SiMe₃ groups in the molecule shown in Figure 1 are twisted in the same direction away from perfect staggering in our model: anticlockwise, when viewed looking toward the Cu₄N₄ core. Thus, the molecular symmetry is approximately D_4 (422), in contrast to the approximate D_{4h} ($4/mmm$) symmetry of the Cu₄N₄ core. The SiMe₃ groups in the other molecule in the unit cell, the mirror image of the one illustrated in Figure 1, are twisted in the opposite direction. The higher-symmetry $I2/m$ model, to give molecular C_{2h} ($2/m$) symmetry, requires either all fully staggered conformations or disorder between groups twisted clockwise and anticlockwise. If our model were superimposed on its mirror image, two sets of C atom positions would result; modeling them with a single set of C atoms with C_{2h} molecular symmetry would lead to large displacement parameters. This is exactly what was reported by Miele et al.:¹⁵ their U_{eq} values for the Cu, N, and Si atoms are very similar to ours, but for the C atoms they are 2–3 times as large. Imposition of centrosymmetry on the molecule constrains the conformations of the SiMe₃ groups in a similar manner, hence the poor results for our refinement in $P2_1/n$.

In summary, the present model is more consistent than the previous one with the actual diffracted intensities (i.e. primitive rather than centered) and leads to a significantly more reasonable chemical picture for the molecule in terms of intramolecular nonbonded contacts.

Electronic Spectra. Electronic absorption and emission spectra for [CuN(SiMe₃)₂]₄ are shown in Figure 2. The cluster is colorless, though it turns pale blue on prolonged exposure to air, probably due to partial oxidation to copper(II). The first two absorption maxima are those shown in Figure 2, at 283 ($\epsilon = 1.65 \times 10^4$) and 246 nm ($\epsilon = 1.7 \times 10^4 \text{ M}^{-1} \text{ cm}^{-1}$); no other bands are apparent at longer wavelengths even in more concentrated solutions.

One of the most striking features of this cluster is its intense blue-green luminescence, which appears when the complex is excited at wavelengths below ca. 400 nm. Corrected emission spectra, also shown in Figure 2, are very similar for the solid and CH₂Cl₂ solution at room temperature and for the solid at 77 K. The corrected excitation spectrum in the 250–400 nm

(23) Brock, C. P.; Dunitz, J. D. *Chem. Mater.* **1994**, *6*, 1118–1127.

(24) Chernikova, N. Yu.; Bel'skii, V. K.; Zorkii, P. M. *J. Struct. Chem.* **1990**, *31*, 661–666.

(25) Johnson, C. K. *Ortep-II: A Fortran Thermal-Ellipsoid Plot Program for Crystal-Structure Illustrations*, Report ORNL-5138; National Technical Information Service, U.S. Department of Commerce: Springfield, VA, 1976.

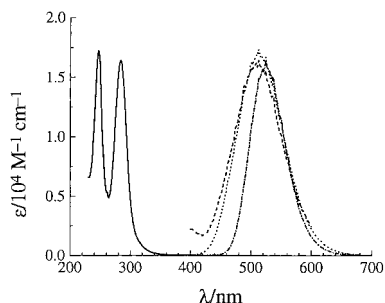


Figure 2. Electronic spectra of $[\text{CuN}(\text{SiMe}_3)_2]_4$: absorption, —, 300 K, CH_2Cl_2 solution; corrected phosphorescence, - - -, 300 K, CH_2Cl_2 solution; ···, 300 K, solid; - · -, 77 K, solid.

Table 4. Phosphorescence Lifetimes for $[\text{CuN}(\text{SiMe}_3)_2]_4^a$

medium	temp/K	lifetime/ μs
CH_2Cl_2 (aerated)	300	1.4
CH_2Cl_2 (degassed)	300	30
solid	300	30
Et_2O (glass)	77	690

^a $\pm 10\%$.

region for a dilute solution of the cluster is essentially identical to the absorption spectrum. The major difference observed at low temperature is that the emission band becomes narrower: full width at half-maximum (fwhm) 2400 cm^{-1} , vs 3500 cm^{-1} at 300 K.

Luminescence lifetimes can also be measured for the cluster by irradiation with a pulsed N_2 laser. Results of these measurements are summarized in Table 4. Two aspects of the data are of interest: first, in room temperature solution, the lifetime is highly sensitive to the presence of O_2 ; and second, the lifetime is considerably longer at 77 K.

Chemical Vapor Deposition. The original report of the synthesis of $[\text{CuN}(\text{SiMe}_3)_2]_4$ describes its purification by sublimation at $180\text{ }^\circ\text{C}$ and 0.2 Torr. Thus, it is much less volatile than the commonly used copper CVD precursors. (By comparison, $\text{Cu}(\text{hfac})_2$ has a vapor pressure of ca. 8 Torr at $100\text{ }^\circ\text{C}$.²⁶) Nevertheless, the cluster's attractive photophysical properties suggested that it might be useful in photochemical deposition of Cu. As a first step toward such photochemical processes, we decided to determine whether $[\text{CuN}(\text{SiMe}_3)_2]_4$ can be used as a precursor for conventional (thermal) Cu CVD.

In typical CVD experiments,¹ the precursor is warmed in an evaporator, under a current of carrier gas, and its vapor is then transported to the reactor, where the substrate is held at a higher temperature to induce deposition. For example, when $\text{Cu}(\text{hfac})_2$ is used as a CVD precursor, it is usually evaporated at $70\text{--}100\text{ }^\circ\text{C}$, and Cu deposition occurs with H_2 carrier gas at substrate temperatures of $200\text{ }^\circ\text{C}$ and higher. However, in the present case, the low volatility of $[\text{CuN}(\text{SiMe}_3)_2]_4$ meant that the required minimum temperature for evaporation might be close to that for deposition; also, it was likely to be difficult to transport the precursor vapor over long distances.

Initial experiments were performed with the precursor in a glass tube inside a tube furnace. With this apparatus, we observed no changes in the precursor when the temperature was kept at $160\text{ }^\circ\text{C}$ or below. At $180\text{ }^\circ\text{C}$, some sublimed (but otherwise unchanged) precursor could be observed on the cool tube walls at the downstream end of the furnace. In contrast, treatment at $200\text{ }^\circ\text{C}$ resulted in deposition of a Cu metal film

near and downstream of the precursor. At these higher temperatures, some sublimation occurred as well, and after the deposition, the residual precursor showed some discoloration. At temperatures above $220\text{ }^\circ\text{C}$, decomposition of the precursor was extensive.

Cu films deposited as described above appeared metallic, but they were otherwise difficult to analyze. Therefore, we also carried out depositions in a warm-wall pedestal reactor, with the precursor placed directly onto the heated borosilicate glass or Si substrates. Deposition under H_2 at $200\text{ }^\circ\text{C}$ (2.5 h) in this apparatus produced metallic films under and around the precursor that were $40\text{--}170\text{ nm}$ in thickness, as determined by stylus profilometry. These films were too thin for analysis by electrical (resistivity) methods. However, powder X-ray diffraction showed that the major component of the films was Cu and that other possible crystalline phases (e.g. CuO , Cu_2O) were absent.

Deposition of Cu films was also observed with this apparatus at lower substrate/evaporation temperatures, although at lower rates: temperatures as low as $145\text{ }^\circ\text{C}$ (H_2 ; 1 atm; 3 h) led to the formation of noticeable metallic Cu films when Si (with native oxide) was used as the substrate. These films formed only directly underneath the precursor, and although they were clearly metallic, they were too thin for analysis by other methods.

Experiments with photoinduced Cu deposition utilized the same apparatus and Si substrates, with the addition of a 150 W Xe arc lamp as light source. The deposition apparatus was made from borosilicate glass, restricting the light transmitted to the sample to wavelengths longer than ca. 300 nm. This, combined with the region of intense absorptions of the cluster, namely, below ca. 350 nm, indicates that the principal irradiation wavelengths were in the $300\text{--}350\text{ nm}$ range under our conditions. When the precursor was irradiated while being held at temperatures below $135\text{ }^\circ\text{C}$, some discoloration occurred but no Cu film deposition. However, at $136\text{--}138\text{ }^\circ\text{C}$ (H_2 ; 1 atm; 3 h), a small amount of Cu film formed. Thus, the minimum substrate temperature for Cu deposition with this precursor is slightly lower under near-UV irradiation than in the dark.

Discussion

Structure of $[\text{CuN}(\text{SiMe}_3)_2]_4$ and Related Compounds.

There are two common geometries for tetranuclear copper clusters. One is the (approximately) planar $\text{Cu}_4(\mu\text{-X})_4$ type reported herein.

X-ray analyses have been performed for a number of $\text{Cu}_4(\mu\text{-X})_4$ clusters: $[\text{CuNEt}_2]_4$,²⁷ $[\text{CuNMe}_2]_4$, and several other Cu(I) amide tetramers,²⁸ $[\text{CuN}(\text{SiMe}_2\text{Ph})_2]_4$,²⁹ $[\text{CuCH}_2\text{SiMe}_3]_4$,³⁰ and $[\text{CuOCMe}_3]_4$.³¹ One other Cu(I) amide, $[\text{CuN}(\text{SiMe}_2\text{Ph})_2]_3$, is a trigonal-planar trimer,²⁹ likely because the trimeric structure minimizes repulsions between the exceptionally bulky $\text{N}(\text{SiMe}_2\text{Ph})_2$ groups. In most of the $\text{Cu}_4(\mu\text{-X})_4$ structures, the Cu and X atoms are approximately coplanar, but $[\text{CuNEt}_2]_4$ ²⁷ and $[\text{CuN}(\text{SiMe}_2\text{Ph})_2]_4$ ²⁹ have a distinct butterfly shape, with the Cu atoms approximately coplanar and the N atoms alternating above and below this plane. Thus, the Cu_4N_4 core in the

(27) Hope, H.; Power, P. *Inorg. Chem.* **1984**, *23*, 936–937.

(28) Gambarotta, S.; Bracci, M.; Floriani, C.; Chiesi-Villa, A.; Guastini, C. *J. Chem. Soc., Dalton Trans.* **1987**, 1883–1888.

(29) Chen, H.; Olmstead, M. M.; Shoner, S. C.; Power, P. P. *J. Chem. Soc., Dalton Trans.* **1992**, 451–457.

(30) (a) Jarvis, J. A. J.; Kilbourn, B. T.; Pearce, R.; Lappert, M. F. *J. Chem. Soc., Chem. Commun.* **1973**, 475–576. (b) Jarvis, J. A. J.; Pearce, R.; Lappert, M. F. *J. Chem. Soc., Dalton Trans.* **1977**, 999–1003.

(31) Greiser, T.; Weiss, E. *Chem. Ber.* **1976**, *109*, 3142–3146.

(26) Temple, D.; Reisman, A. H. *J. Electrochem. Soc.* **1989**, *136*, 3525–3529. Wolf, W. R.; Sievers, R. E.; Brown, G. H. *Inorg. Chem.* **1972**, *11*, 1995–2002.

“butterfly” clusters has approximate D_{2d} , or $\bar{4}2m$ symmetry, vs D_{4h} , $4/mmm$, in $[\text{CuN}(\text{SiMe}_3)_2]_4$.

The distances and angles in the Cu_4N_4 core of $[\text{CuN}(\text{SiMe}_3)_2]_4$ are similar to those for the other amide tetramers. As Hope and Power observed for $[\text{CuNEt}_2]_4$,²⁷ the distances in the amides are intermediate between those found for the Cu_4C_4 core of $[\text{CuCH}_2\text{SiMe}_3]_4$ (Cu–X longer, $\text{Cu}\cdots\text{Cu}$ shorter)³⁰ and for the Cu_4O_4 core of $[\text{CuOCMe}_3]_4$ (Cu–X shorter, $\text{Cu}\cdots\text{Cu}$ longer).³¹ This trend in Cu–X distances is expected as a consequence of atomic size ($\text{O} < \text{N} < \text{C}$). The opposite trend in $\text{Cu}\cdots\text{Cu}$, although initially somewhat surprising, may reflect the increasing total coordination number at the bridging X ligand in the order $[\text{CuOCMe}_3]_4$ (3) < $[\text{CuNR}_2]_4$ (4) < $[\text{CuCH}_2\text{SiMe}_3]_4$ (5). The five coordination at the bridging alkyl C atoms in $[\text{CuCH}_2\text{SiMe}_3]_4$, for example, probably causes the smaller Cu–X–Cu angle, which in turn accommodates the larger Cu–X distance and permits a closer $\text{Cu}\cdots\text{Cu}$ approach.

The other important family of Cu^{I} clusters is the “cubane” type, $[\text{LCu}-\mu_3\text{-X}]_4$, of idealized symmetry T_d , in which the metal and triply bridging X occupy alternate corners in a cube. For example, although $[\text{CuOCMe}_3]_4$ is square, as discussed above, its CO adduct has the cubane-type structure, $[(\text{OC})\text{Cu}-\mu_3\text{-OCMe}_3]_4$.³² The cubane clusters are structurally substantially different from the present compound, $[\text{CuN}(\text{SiMe}_3)_2]_4$, but they are also of interest because several of them, including $[\text{LCuI}]_4$ (L = pyridine, piperidine) are photoactive.

Electronic Structure. Excited states of copper(I) complexes are of three types, interconfigurational, intraligand, and MLCT; the d^{10} configuration makes d–d and LMCT excited states impossible.¹² For $[\text{CuN}(\text{SiMe}_3)_2]_4$, low-energy intraligand transitions are unlikely: the lowest-energy electronic absorption band in hexamethyldisilazane, $\text{HN}(\text{SiMe}_3)_2$, is at 203 nm.³³ MLCT transitions cannot be conclusively ruled out, but the ligand LUMOs, probably the Si d orbitals, are likely to be at high energy. (Also, in the electronic spectrum of $\text{HN}(\text{SiMe}_3)_2$, the position of the first absorption maximum has been reported not to be highly solvent-sensitive.³³ This argues against an assignment involving charge transfer to Si.) Thus, the low-energy absorption and emission bands in this cluster are likely to be due to transitions primarily localized on the Cu atoms.

In simple mononuclear Cu(I) complexes, interconfigurational transitions are commonly observed. For example, in the absorption spectra of monomeric $\text{M}(\text{PPh}_3)_3$ complexes (M = Pd, Pt), intense UV absorptions have been assigned to $3d_{x^2-y^2} \rightarrow 4p$ transitions.³⁴ However, in the present cluster, the $\text{Cu}\cdots\text{Cu}$ distances (ca. 2.7 Å; see Table 3) are less than twice the Cu van der Waals radius (1.43 Å³⁵). Thus, it is likely that the cluster electronic states will involve substantial metal–metal interaction.³⁶

Referring to the coordinate system in Figure 3, the Cu orbitals most likely to interact strongly with one another are the $3d_{x^2-y^2}$ (filled) and $4s$ and $4p_x$ (empty). These Cu atomic orbitals will combine to form three sets of MOs, each comprising a_{1g} , bonding; e_u , approximately nonbonding; and b_{1g} , antibonding

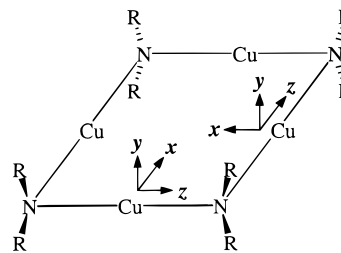


Figure 3. Coordinate systems for Cu atoms in $[\text{CuN}(\text{SiMe}_3)_2]_4$ (R = SiMe_3). Cu p_x orbitals are expected to show maximum $\text{Cu}\cdots\text{Cu}$ interaction. See text for details.

(in idealized D_{4h} symmetry). The cluster LUMO is likely to be one of the a_{1g} combinations with a substantial contribution from Cu $4p_x$ AOs. (The HOMO may be a b_{1g} combination derived from $d_{x^2-y^2}$ AOs.)

The very long luminescence lifetime we observe for $[\text{CuN}(\text{SiMe}_3)_2]_4$ luminescence, 30 μs even in solution at room temperature, argues in favor of phosphorescence. The large Stokes shift between the emission and first absorption maxima in $[\text{CuN}(\text{SiMe}_3)_2]_4$ (ca. 15 800 cm^{-1} in CH_2Cl_2) may be due to a combination of two factors. First, if the lowest-energy excited state of the cluster involves population of an orbital with metal–metal bonding character, such as the empty $a_{1g}(4p_x)$ MO mentioned above, this could make the $\text{Cu}\cdots\text{Cu}$ distances significantly shorter in the excited state than in the ground state, leading to an unusually large Stokes shift. This behavior would be similar to that of the tetranuclear gold(I) clusters $[\text{Au}(\text{S}_2\text{CCH}_3)]_4$ and $[\text{AuCl}(\text{pip})]_4$ (pip = piperidine): in these complexes, large Stokes shifts between absorption and emission have been attributed to substantial shortening of $\text{Au}\cdots\text{Au}$ distances in the excited state.³⁷ Second, if the HOMO is b_{1g} , as suggested above, then the lowest-energy spin-allowed transition, ${}^1A_{1g} \rightarrow {}^1B_{1g}$ ($b_{1g}(3d_{x^2-y^2}) \rightarrow a_{1g}(4p_x)$) is electric-dipole-forbidden. This would make it weak and possibly difficult to observe in absorption. Then the first fully allowed transition, responsible for one of the intense absorptions in the UV, would be ${}^1A_{1g} \rightarrow {}^1E_u$ (e.g. $b_{1g}(3d_{x^2-y^2}) \rightarrow e_u(4p_x)$). These would be higher in energy than the HOMO–LUMO transition, increasing the Stokes shift still further.³⁸

In addition to the polypyridine and phosphine species discussed in the Introduction, other examples of luminescent copper(I) complexes include the “cubane” clusters $[(\text{pip})\text{CuI}]_4$ and $[(\text{py})\text{CuI}]_4$ (py = pyridine).³⁹ Ford and co-workers have identified phosphorescent metal-centered (i.e. interconfigurational) excited states in both of these species, as well as an emissive interligand ($\text{I} \rightarrow \text{py}$ charge-transfer) state in the pyridine complex.⁴⁰ Phosphorescent copper(I) cluster ions containing phosphine and sulfur ligands have been reported recently and their excited-state redox reactions studied.⁴¹ Extended solids containing adducts of copper(I) halides have been shown to be luminescent.⁴² Interconfigurational phosphorescence has been

(37) Vogler, A.; Kunkely, H. *Chem. Phys. Lett.* **1988**, *150*, 135–137.

(38) If the prominent absorption and emission bands are associated with different electronic transitions, we might expect to find some evidence in the cluster’s absorption spectrum (300–500 nm) for the spin-allowed partner of the phosphorescence transition. We found no such evidence, even in more concentrated solutions, although these experiments were limited somewhat by the low solubility of the cluster in common solvents.

(39) Vogler, A.; Kunkely, H. *J. Am. Chem. Soc.* **1986**, *108*, 7211–7212.

(40) Vitale, M.; Palke, W. E.; Ford, P. C. *J. Phys. Chem.* **1992**, *96*, 8329–8336. See also: Kyle, K. R.; Ryu, C. K.; DiBenedetto, J. A.; Ford, P. C. *J. Am. Chem. Soc.* **1991**, *113*, 5132–5137.

(41) Yam, V. W.-W.; Lee, W.-K.; Lai, T.-F. *J. Chem. Soc., Chem. Commun.* **1993**, 1571–1573.

(32) Geerts, R. L.; Huffman, J. C.; Foltling, K.; Lemmen, T. H.; Caulton, K. G. *J. Am. Chem. Soc.* **1983**, *105*, 3503–3506.

(33) Pitt, C. G.; Fowler, M. S. *J. Am. Chem. Soc.* **1967**, *89*, 6792–6793. Kirichenko, E. A.; Ermakov, A. I.; Pimkin, N. I.; Andrianov, K. A.; Kopylov, V. M.; Shkol’nik, M. I. *J. Gen. Chem. USSR* **1979**, *49*, 1333–1336.

(34) Harvey, P. D.; Gray, H. B. *J. Am. Chem. Soc.* **1988**, *110*, 2145–2147.

(35) Porterfield, W. W. *Inorganic Chemistry: A Unified Approach*, 2nd ed.; Academic Press: New York, 1993; p 214.

(36) We thank a reviewer for alerting us to the likely importance of metal–metal interactions in this cluster.

observed from simple copper(I) species such as CuCl_3^{2-} ⁴³ and $\text{NaF}:\text{Cu}^+$.⁴⁴ Finally, a recent report describes an unusual example of *fluorescence* from a copper(I) complex, the bridged dimer $\text{Cu}_2(\text{PhNNNPh})_2$.⁴⁵ (In this case, however, the triazene ligands have extensive π systems, and the fluorescence appears to be primarily ligand-localized.)

The $[\text{CuN}(\text{SiMe}_3)_2]_4$ excited-state decay rate increases by about a factor of 20 in air-saturated solutions (see lifetimes in Table 4). This indicates efficient quenching of the cluster's phosphorescent excited state by O_2 : the quenching rate constant is likely to be greater than $10^8 \text{ M}^{-1} \text{ s}^{-1}$.⁴⁶ This is comparable to rate constants for reaction of excited $\text{Ru}(\text{bpy})_3^{2+}$ with O_2 : $6.8 \times 10^8 \text{ M}^{-1} \text{ s}^{-1}$ in CHCl_3 ⁴⁷ and $1.8 \times 10^9 \text{ M}^{-1} \text{ s}^{-1}$ in $\text{CH}_3\text{-OH}$.⁴⁸

Deposition of Copper. The very low volatility of the $[\text{CuN}(\text{SiMe}_3)_2]_4$ cluster makes extensive CVD studies difficult, because the temperature required for significant vaporization of the compound (ca. 180 °C) is close to its decomposition temperature.

We observed two types of behavior at higher evaporation temperatures with this precursor under H_2 carrier gas. At ca. 180 °C, some evaporation occurred, as indicated by the collection of some white luminescent sublimate downstream from the heated zone; but no reduction to Cu occurred. At 200 °C, both precursor sublimation and Cu film deposition occurred. At the higher temperature the residual $[\text{CuN}(\text{SiMe}_3)_2]_4$ precursor also began to discolor during the deposition, to a yellowish-brown color. The Cu films that are produced under these conditions are not of high quality, but they are clearly metallic; some of the discoloration in the films, as well as their nonuniformity, may be due to the deposition geometry (i.e. evaporation and deposition areas in close proximity).

To determine whether the attractive photophysical properties of $[\text{CuN}(\text{SiMe}_3)_2]_4$ could be combined with the above CVD behavior, we carried out deposition experiments under Xe arc lamp irradiation, all under 1 atm H_2 . With evaporation and deposition temperatures of 180 °C and higher, as outlined above,

irradiation had no obvious effect on deposition rates. Therefore, we also performed experiments at lower temperatures. We discovered that small amounts (visible metallic films after 3 h) of Cu deposition occurred on Si substrates in the dark with evaporation/substrate temperatures as low as 145 °C. Due to the very low vapor pressure of the precursor at these temperatures, this deposition occurred only directly beneath the solid precursor. This lower-temperature deposition process is slightly photosensitive: with Xe lamp irradiation, metallic films form at 136–138 °C.

Our best CVD results were obtained with Si substrates. This is similar to the work of Chisholm and co-workers,¹⁴ who succeeded in depositing Cu films on Si (but not on quartz or glass) using $[\text{CuN}(\text{SiMe}_3)_2]_4$ as precursor. There are two differences between our work and the earlier one: First, we are able to use significantly lower substrate temperatures. This may be due to our use of H_2 as reducing carrier gas, as compared with the previous work, which was done at low pressure, without carrier gas. Second, we have demonstrated a small but measurable photochemical effect on our deposition process.

Conclusions

The square-planar tetrameric copper(I) cluster $[\text{CuN}(\text{SiMe}_3)_2]_4$ is intensely phosphorescent. The lifetime of this emission, which is likely to be associated with a metal-centered transition, is long and highly sensitive to the presence of dissolved O_2 . Although the cluster has very low volatility, it is nevertheless possible to use it as a precursor in a simple CVD reactor for deposition of copper metal. Furthermore, this CVD process can be enhanced photochemically. Experiments now in progress include extending the chemical and photochemical vapor deposition experiments to other copper(I) amide clusters (for example, other Cu(I) amides,⁴⁹ as well as the cluster $[\text{CuCH}_2\text{-SiMe}_3]_4$,³⁰ have been reported to be photosensitive), and chemical modifications that may lead to photophysically similar but monomeric (and thus more volatile) species.

Acknowledgment. A.M.J. thanks the Louisiana Board of Regents for a graduate fellowship. We thank Drs. R. H. Schmehl and R. Ferrell for assistance with lifetime and powder-diffraction measurements and Drs. G. L. Griffin and B. Koplitz for numerous helpful discussions. This work was supported by the Department of Energy (EPSCoR) and the National Science Foundation (Grants CTS-9311527 and CTS-9612157).

Supporting Information Available: X-ray structural data for $[\text{CuN}(\text{SiMe}_3)_2]_4$ at 130 and 296 K, in CIF format, are available on the Internet only. Access information is given on any current masthead page.

IC971341P

- (42) Rath, N. P.; Holt, E. M.; Tanimura, K. *Inorg. Chem.* **1985**, *24*, 3934–3938. Rath, N. P.; Holt, E. M.; Tanimura, K. *J. Chem. Soc., Dalton Trans.* **1986**, 2303–2310. Jasinski, J. P.; Rath, N. P.; Holt, E. M. *Inorg. Chim. Acta* **1985**, *97*, 91–97.
- (43) Stevenson, K. L.; Braun, J. L.; Davis, D. D.; Kurtz, K. S.; Sparks, R. I. *Inorg. Chem.* **1988**, *27*, 3472–3476.
- (44) Payne, S. A.; Goldberg, A. B.; McClure, D. S. *J. Chem. Phys.* **1983**, *78*, 3688–3697.
- (45) Harvey, P. D. *Inorg. Chem.* **1995**, *34*, 2019–2024.
- (46) We were unable to find data for the solubility of O_2 in CH_2Cl_2 . We estimate a value of 0.008 M at 1 atm and 25 °C, on the basis of data for CHCl_3 and CCl_4 tabulated in: Linke, W. F. *Solubilities of Inorganic and Metal-Organic Compounds*; American Chemical Society, Washington, DC, 1965; Vol. 2, p 1234. This estimate leads to an O_2 quenching rate constant of $3 \times 10^8 \text{ M}^{-1} \text{ s}^{-1}$.
- (47) Timpson, C. J.; Carter, C. C.; Olmsted, J., III. *J. Phys. Chem.* **1989**, *93*, 4116–4120.
- (48) Demas, J. N.; Harris, E. W.; McBride, R. P. *J. Am. Chem. Soc.* **1977**, *99*, 3547–3551.

- (49) Yamamoto, T.; Ehara, Y.; Kubota, M.; Yamamoto, A. *Bull. Chem. Soc. Jpn.* **1980**, *53*, 1299–1302.